Heliyon 10 (2024) e36113

Contents lists available at ScienceDirect

Heliyon

journal homepage: www.cell.com/heliyon

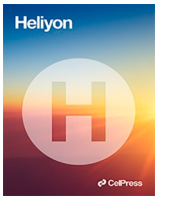

Research article

# Reactive extraction of muconic acid by hydrophobic phosphonium ionic liquids - Experimental, modelling and optimisation with Artificial Neural Networks

Alexandra Cristina Blaga [a,*], Elena Niculina Dragoi [a], Alexandra Tucaliuc [a], Lenuta Kloetzer [a], Adrian-Catalin Puitel [a], Dan Cascaval [a,**], Anca Irina Galaction [b]

[a] "Gheorghe Asachi" Technical University of Iasi, "Cristofor Simionescu" Faculty of Chemical Engineering and Environmental Protection, Iasi, Romania

[b] "Grigore T. Popa" University of Medicine and Pharmacy, Faculty of Medical Bioengineering, Iasi, Romania

ARTICLE INFO

*Keywords:*
Reactive extraction
Mathematical modelling
Ionic liquid
Muconic acid
[$C_{14}C_6C_6C_6P$][Dec]

ABSTRACT

Muconic acid is a six-carbon dicarboxylic acid with conjugated double bonds that finds extensive use in the food (additive), chemical (production of adipic acid, monomer for functional resins and bio-plastics), and pharmaceutical sectors. The biosynthesis of muconic acid has been the subject of recent industrial and scientific attention. However, because of its low concentration in aqueous solutions and high purity requirement, downstream separation presents a significant problem. Artificial Neural Networks and Differential Evolution were used to optimize process parameters for the recovery of muconic acid from aqueous streams in a system with n-heptane as an organic diluent and ionic liquids as extractants. The system using 120 g/L tri-hexyl-tetra-decyl-phosphonium decanoate dissolved in n-heptane, pH of the aqueous phase 3, 20 min contact time, and 45 °C temperature assured a muconic acid extraction efficiency of 99,24 %. Low stripping efficiency compared to extraction efficiency was observed for the optimum conditions on the extraction step (120 g/L ionic liquids dissolved in heptane). However, re-extraction efficiencies obtained for the recycled organic phase in three consecutive stages were close to the first extraction stage. The mechanism analysis proved that the analysed phosphonium ionic liquids (PILSs) extracts only undissociated molecules of muconic acid through H-bonding.

## 1. Introduction

Muconic acid, MA, is a versatile building block with various applications: is an essential intermediate in the synthesis of adipic acid, a precursor for the production of bio-based polymers such as polyethylene terephthalate (PET) and polybutylene terephthalate (PBT), as the building block for the synthesis of various speciality chemicals: adipic dihydrazide, hexamethylene diamine, and cyclohexane-dicarboxylic acid, as a starting material for the production of bioplastics and biofuels [1–3]. It can be converted into renewable chemicals and materials through bio-based processes, contributing to a more sustainable and environmentally friendly approach.

* Corresponding author. "Gheorghe Asachi" Technical University of Iasi, "Cristofor Simionescu" Faculty of Chemical Engineering and Environmental Protection, D. Mangeron Av., no 67, Iasi, Romania.

** Corresponding author.

*E-mail addresses:* acblaga@tuiasi.ro (A.C. Blaga), dan.cascaval@academic.tuiasi.ro (D. Cascaval).

https://doi.org/10.1016/j.heliyon.2024.e36113
Received 8 May 2024; Received in revised form 17 July 2024; Accepted 9 August 2024
Available online 10 August 2024

**Table 1**
Production of muconic acid through biosynthesis.

| Microorganism | Process | MA produced | Ref. |
|---|---|---|---|
| Engineered *Saccharomyces cerevisiae* | Fed-batch cultivation through the shikimate pathway<br>40 g/L glucose | 1.2 g/l MA under prototrophic conditions<br>5.1 g/l MA when supplemented with amino acids | [6] |
| Engineered *Saccharomyces cerevisiae* ST10209 | Fed-batch fermentation (50 L bioreactor)<br>10 g/L yeast extract | 15.2 g/L (muconate) | [7] |
| Engineered *Escherichia coli* | Fed-batch fermentation<br>20 g/L glucose | 3.153 ± 0.149 g/L | [8] |
| Engineered *Escherichia coli* | Batch fermentation<br>20 g/L glucose | 4.45 g/L | [9] |
| Engineered *Corynebacterium glutamicum* | Fed-batch fermentation through 3-dehydroshikimate (DHS) pathway<br>55 g/L glucose | 53.8 ± 5.5 g/L (muconate) | [10] |
| Engineered *Pseudomonas chlororaphis* HT66 | Fed-batch fermentation<br>18 g/L glycerol | 3.376 g/L | [11] |
| Engineered *Pseudomonas putida* | Fed-batch fermentation<br>10.6 g/L glucose | Strain LC224:<br>26.8 g/L (muconate)<br>Strain QP478:<br>9.3 g/L (muconate) | [12] |
| Engineered *Klebsiella pneumoniae* | Flask cultivation<br>80 g/L of glucose | 2.1 g/L | [13] |
| Engineered *Pichia occidentalis* LP635 | Fed-batch fermentation<br>40 g/L glucose | 38.8 g/L (muconate) | [14] |

MA production is an active area in research and development, and new methods and technologies must be explored to improve the production process's efficiency, yield, and sustainability. MA can be produced through different processes, including both chemical and biological methods: chemical synthesis from benzene through a multi-step process or biological production from renewable feedstocks [4,5]. In chemical synthesis, benzene is first converted to catechol through a series of reactions. Then, catechol is oxidized to muconic acid, a process involving various chemical reagents and catalysts. Through microbial fermentation (Table 1), muconic acid can be produced using mainly glucose or glycerol as a carbon source.

MA separation from fermentation broth is realized through multiple steps, with high costs and important consumption of materials. Yoshikawa et al. suggested a multistep separation approach that involves filtering, adsorption/desorption, precipitation, ion exchange chromatography, and sedimentation to produce MA with a 95 % purity and 90 % yield [15]. Kohlstedt used catechol and p-coumaric acid as the substrates for the bioconversion of MA (cis-cis) in *Pseudomonas putida* fermentation. For the downstream part, the fermentation broth was treated with activated carbon to remove coloured compounds and proto-catechuic acid. MA was precipitated at pH 2 (32 % HCl) and 5 °C temperature, and spray drying (50 °C) was used as a recovery and purification step. Overall recovery yield was 74 %, and the resulting MA had a purity level higher than 97 % [16]. The traditional approaches have drawbacks such as waste production, excessive energy consumption, and material requirements that drive up expenses. Given that the downstream recovery process for most carboxylic acids accounts for 30–50 % of the total production cost [17], developing an efficient separation and recovery procedure for muconic acid is critical to minimizing costs.

Reactive extraction is utilized in various industries for purification and separation of chemicals: extraction of metals from ores, removal of impurities from solutions, recovery of valuable compounds, and transformation of chemical species into more desirable forms. For carboxylic acids, the reactive extraction process involves two immiscible phases: an aqueous phase that includes the acid and an organic phase that contains a complexing extractant. The critical step of the process is the reversible formation of a complex carboxylic acid-extractant, which is soluble in the organic phase. After the separation process is completed, the extractant is recovered from the complex by increasing the temperature or adding sodium hydroxide/sodium carbonate solutions [18]. The choice of solvents, extractants, and operating conditions depends on the specific application and the solute-solvent systems' properties. For muconic acid separation, several solvents were analysed, obtaining low extraction efficiency: 26.23 % for hexane, and 36.17 % for methyl isobutyl ketone [19]. Adding amines into the organic phase in a system with ethyl oleate, 1-dodecanol, and di-n-octylamine increased the extraction efficiency to 98.66 % [20]. Bahrami et al. (2018) analysed a supported hollow liquid membrane containing 1-octanol and 10 % w/v of Aliquat 336 for trans,trans-MA (benzene metabolite) extraction from human urine and stripping using a solution containing 3.0 mol/L sodium chloride, obtaining 87–95 % recovery [20]. Abbaszadeh et al. (2021) analysed an in-syringe ionic liquid-dispersive liquid-liquid microextraction process for preconcentration of trans,trans-MA in the human urine sample, using trihexyl(tetradecyl)phosphonium chloride as an easy and rapid analysis of low amounts of urinary t,t-MA with HPLC-UV [21]. A highly efficient and biocompatible approach of reactive extraction was developed by Tonjes et al. (2023) using 12.5 % (v/v) CYTOP 503 dissolved in canola oil in a direct extraction procedure from *Saccharomyces cerevisiae MDS130* fermentation broth, which laid the foundation for the environmentally friendly production of MA. The method was successfully realized in a fed-batch fermentation (10 L bioreactor volume), with a final MA titer of 4.33 g/L and the highest achieved productivity of 0.053 g/L [22,23].

The current methods of separating MA have several drawbacks, including low extraction efficiencies and increased prices for the finished product due to the high complexity of the separation procedures (such as chromatography), which also require extensive time and energy. Moreover, hazardous volatile chemical solvents are typically used. Due to these drawbacks, it is necessary to develop

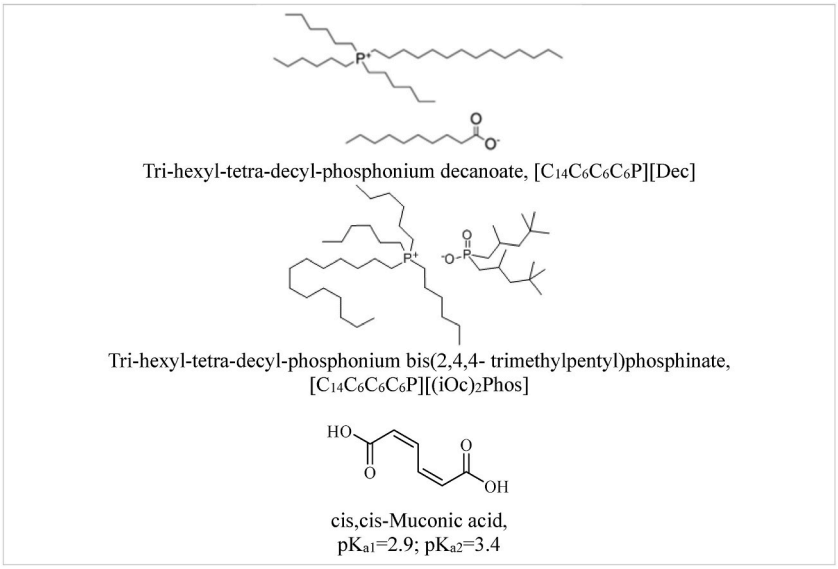


**Fig. 1.** Chemical structure of muconic acid and PILs used in this study.

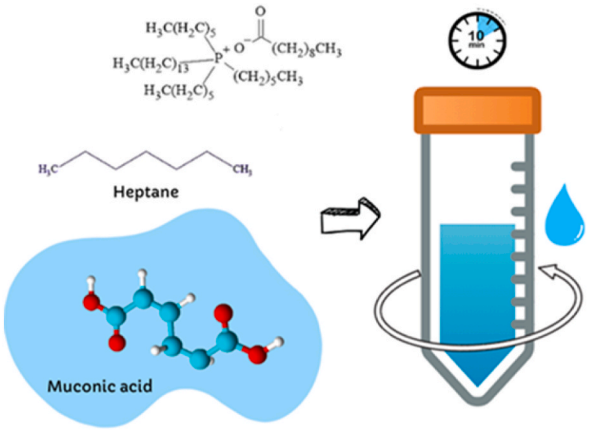


**Fig. 2.** Schematic representation of extraction step.

"greener" and more sustainable extraction and purification methods; one such method that has drawn interest is the use of ionic liquids (ILs), due to their excellent solvation ability. ILs have been proposed as promising extractants for carboxylic acids, such as lactic, butyric, and acetic [24–26].

Physical or mathematical modelling is vital in separation to correlate input and output design variables, and it may be used in the simulation and optimisation of the separation process to help find an efficient and economical method. Selecting a suitable technique for evaluating different process parameters and any interactions involved while minimizing the number of experimental runs is essential. In recent years, the rapid development of artificial intelligence (AI) techniques, especially of different types of neural networks (ANNs), coupled with advances in computing power, allowed the generation of robust systems that can be efficiently used for various tasks. Examples of ANN (simple or in combination with multiple algorithms) applied for modelling of processes focused on the extraction of various valuable products include: i) betalain pigment extraction from *Beta vulgaris*; a comparison between response surface methodology (RSM), classical one layer ANNs and a hybrid RSM - Genetic Algorithm (GA) approach was performed [27]; ii) bioactive compounds extraction from *Allium sativum* L. leaf powder; two strategies were used for process modelling and optimisation: RSM with a rotable central composite design and a hybrid ANN-GA approach [28]; iii) phycocyanin extraction from *Arthrospira platensis*; RSM with Box-Behnken design and one hidden layer ANN were used for process modelling and optimisation [29]; iv) ellagitannins extraction from black raspberry seeds; a one hidden layer with ten neurons ANN trained with Levenberg Marquardt and coupled with GA was used [30]; pseudomonic acids extraction; a shallow ANN model combined with DE, BackPropagation algorithm and a Local Search procedure was used to model and optimize the process [31]. While relatively easy to use, the AI-based systems must be prior trained and their optimal settings determined in order to provide good results. This is also applicable for ANNs, where their

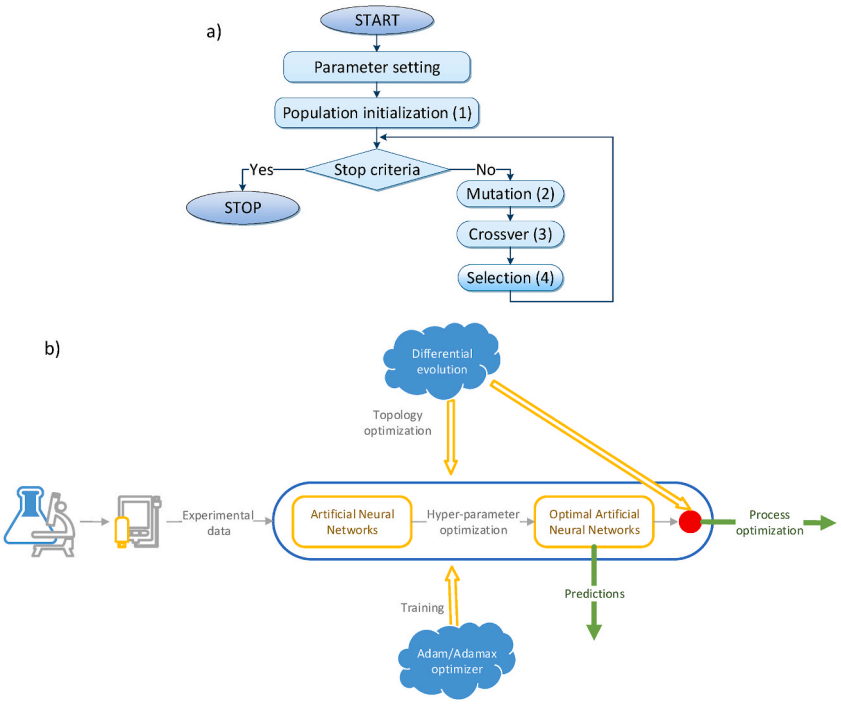


**Fig. 3.** Simplified schema of the a) DE algorithm; b) modeling and optimisation strategy.

topology and internal parameters are still challenging to determine, and the combination of ANN-DE used in this work aims to alleviate some of these challenges. The strategy describing the combination of the two approaches is presented in Section 2.2.

This study aims to search for a feasible downstream processing alternative for MA separation from aqueous media, resulting in an effective extraction system by analyzing two hydrophobic ionic liquids based on tetradecyl-(trihexyl) phosphonium – $[C_{14}C_6C_6C_6P]$: Cyphos IL104 – $[C_{14}C_6C_6C_6P][(iOc)_2Phos]$ and Cyphos IL103 - $[C_{14}C_6C_6C_6P][Dec]$ dissolved in n-heptane.

A thorough analysis was conducted of the variables influencing the extraction behaviour of MA, including temperature, aqueous phase pH, type and concentration of extractant, and contact time. The process was modelled and optimised using a deep neural network with an optimised structure obtained using the Differential Evolution (DE) algorithm.

## 2. Materials and methods

### 2.1. Chemical and methods

All chemicals, including muconic acid cis-cis (97.0 %), $[C_{14}C_6C_6C_6P][(iOc)_2Phos]$ (95 %), $[C_{14}C_6C_6C_6P][Dec]$ (95 %), heptane (99 %), sodium phosphate (99 %), sodium hydroxide (>97 %), sulfuric acid (95.0–98.0 %), and acetonitrile (99.99 %), were purchased from Sigma and used as received (see Fig. 1).

The experiments performed for MA extraction (Fig. 2.) were carried out using a vibration shaker that ensured a stirring speed of 1200 rpm (extraction time between 10 and 30 min and temperature 25–65 °C), using equal volumes (2 mL) of MA solution, and the organic phase using a glass cell. MA was extracted from aqueous solutions whose initial concentration was 0.8 g/L. The extraction was carried out either using Cyphos IL103 - Trihexyl-tetra-decyl-phosphonium decanoate and Cyphos IL104 - Tri-hexyl-tetra-decyl-phosphonium bis(2,4,4- trimethylpentyl)phosphinate, mixed with n-heptane, the ionic liquid concentration in the organic phase varied between 0 and 120 g/L. The pH of the initial aqueous phase was corrected to the predetermined value, using 4 % sulfuric acid and 4 % sodium hydroxide solutions, based on the indications of a Hanna Instruments pH 213 digital pH meter. The pH of MA solution 0.8 g/L was 3.05 before any adjustment, and its pH at equilibrium was 4.45. After extraction, the samples were separated by centrifugation at 4000 rpm for 5 min. The analysis of the process was carried out using the extraction efficiency, E (%), which was calculated by determining the MA concentration from the initial solution and the raffinate solution using a Dionex Ultimate HPLC system equipped with a Hypersil Gold column, the mobile phase being a mixture of 35 % acetonitrile and 65 % sodium phosphate solution with a flow rate of 0.75 mL/min, detection at 210 nm. The stripping experiments for MA separation were carried out using diluted sodium hydroxide solution (pH 12, modified using the indications of the digital pH meter (CONSORT C 836) in equal volumes with loaded organic phases organic phase (2 mL) using a vibratory shaker with 1200 rpm and 20 min contact time. After extraction, the aqueous exhausted phase was removed, and the organic extract was mixed with the stripping phase. The back extraction efficiency was calculated using the equation:

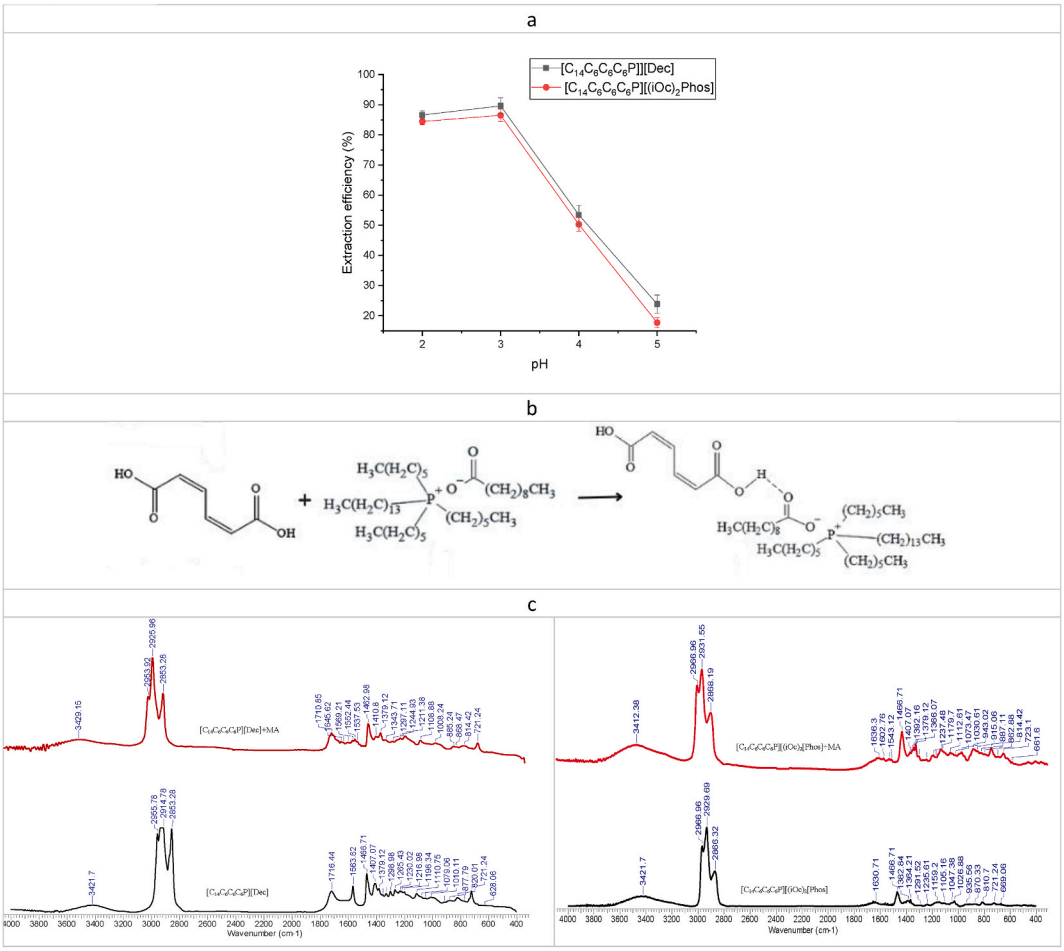


**Fig. 4.** pH influence on MA reactive extraction.

$$S = \left(\frac{C_s}{C_0\text{-}C}\right) \bullet 100, \%$$

where $c_s$, $c_0$, and c (g/L) are MA concentrations in the stripping solution, aqueous initial solutions, and the raffinate (exhausted initial solution after extraction). All experiments were performed in triplicate (n = 3, error between 1.5 and 4.5 %). An Agilent Cary 630 FTIR instrument (32 scans per sample at 4 $cm^{-1}$ spectral resolution and 4000–400 $cm^{-1}$ range) was used for FTIR analysis.

### 2.2. Modelling and optimisation

The process was modelled using a neuro-evolutionary approach in which a sequential multiple-layer ANN model's structure (the number of hidden layers and neurons in each hidden layer) is automatically determined using the DE algorithm. DE is a bio-inspired metaheuristic that has proved its efficiency in solving many problems. Considering the No Free Lunch theorem [32], many optimisers can provide good results for this problem. However, DE was chosen based on its simplicity, reduced number of parameters, and overall performance. As with every population-based algorithm, DE evolves (through a series of steps) a set of randomly generated potential solutions until a stop criterion is reached.

The initial solutions are generated using random number generators following different distribution functions (usually normal distribution) in the initialisation step (step 1). The other steps used by DE include mutation (step 2), crossover (step 3), and selection (step 3). The mutation introduces new information in the population through a specific DE operator called differentiation (in its simple form, to a base individual, a scaled differential term is added). In the crossover step, a new population is created by combining data from the individuals from the current and the mutated populations. The resulting individuals are compared with the existing population, and if their fitness (a measure that indicates their performance) is better, they are selected to form the new population. In this case, the stop criterion is represented by the number of iterations reaching a pre-determined value. The control parameters that direct the search are introduced into the individuals and are modified as the other parameters (the self-adaptation principle). The type of parameters and the mechanisms used in each algorithm step indicate its variant. Fig. 3a presents the simplified schema of the DE

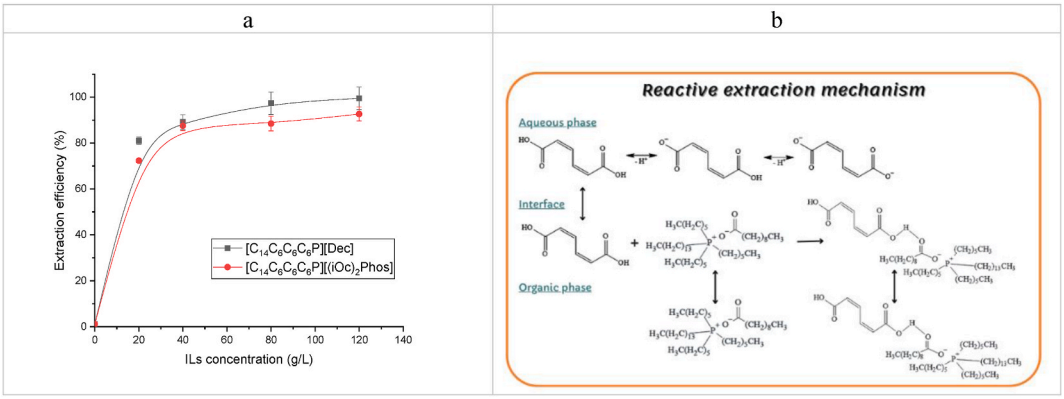


**Fig. 5.** PILs concentration influence on MA reactive extraction (0.8 g/L MA concentration, aqueous phase pH 3, 10 min contact time).

algorithm. The general principles of DE, the mathematical relations describing each step, and the concepts used to combine it with ANNs are described in Ref. [33]. The simplified schema of the modelling and optimisation strategy is presented in Fig. 3b.

The model's training was performed using the algorithms Adam (Adaptive Moment Estimation) and Adamax (Adam variant using infinite norm). Both algorithms are gradient-based variants and incorporate adaptive learning rates that improve efficiency and reduce training time. L1 regulation (also known as Lasso regulation) was applied to prevent overtraining. This involves adding a penalty to the loss function and has the effect of forming model parameters towards small values, thus introducing sparsity. The implementation was done in Python, using the TensorFlow and sklearn modules. The best-resulting models and the Python script for running it can be downloaded from https://elenadragoi.ro/CV/Documents/muconic_model.zip.

## 3. Results and discussion

### 3.1. Influence of various parameters on MA reactive extraction

Because of their hydrophilic nature and their dissociation in aqueous solutions, short-chain carboxylic acids, like MA, cannot be directly recovered in an organic solvent. Instead, if an extractant is added in the organic phase, it can form with MA a hydrophobic complex, soluble mainly in the organic phase. ILs are characterised by exceptional solvation ability, nonflammability, low volatility, and good chemical, thermal, and electrochemical stability. They can be used as extractants and diluents for hydrophilic carboxylic acid separation, which is much safer than conventional organic solvents. Due to their high viscosity, which makes them difficult to utilise alone, they are frequently combined with organic solvents (diluents) to improve extraction effectiveness. n-Heptane has been selected as the inactive diluent for this investigation due to its very low water solubility and good miscibility with PIls. The extraction of MA from aqueous solutions using a mixture of phosphonium ionic liquids - PILs and heptane-was examined using varying aqueous phase pH, time, temperature, and ionic liquid concentration.

The pH of the aqueous phase is a decisive factor in the efficiency of the reactive extraction process. Fig. 4a shows the influence of the aqueous phase pH on the extraction of MA by 40 g/L PIls diluted in n-heptane. The extraction efficiency increases in the pH range of 2–3, being reduced when the pH of the aqueous phase increases above pH 3. Carboxylic acids, in aqueous solutions, can be undissociated at pH lower than pKa ($pKa_1$ 2.9 and $pKa_2$ 3.4 for MA [34]) or dissociated at pH higher than pKa, with the degree of ionisation influencing its solubility and partitioning behaviour between the aqueous and organic phases. The highest extraction efficiency was observed in the experimental data at a pH lower than pKa; when pH increases above $pKa_2$, the acid equilibrium switches to dissociation of both carboxylic groups, and extraction efficiency decreases. Taking into account the characteristics of PILs and MA, the obtained results show that the formation of the complex MA-PIls is based on hydrogen bonds between the ionic liquid and the undissociated form of the MA, as to get optimal extraction efficiency, the pH of the aqueous phase needs to be lower than the $pKa_2$ (3.4). The cis-cis form of MA is in its protonated form at pH 3.4. However, the increase of pH until 6 and an increase in temperature could determine its irreversible conversion of CCM into cis, trans form, which is less available for reacting with PILs. This property can be exploited in the back-extraction step.

The extraction mechanism, presented in Fig. 4b, assumes H-bond formation between the protonated MA and the binding sites in the anion of the IL (for example, the oxygen of bis(2,4,4-trimethylpentyl) phosphinate, in the case of $[C_{14}C_6C_6C_6P][(iOc)_2Phos]$ or from decanoate - carboxylate for $[C_{14}C_6C_6C_6P][Dec]$). Due to extractant protonation, adding sulfuric acid for pH control (at pH 2) slowly decreases the extraction efficiency and PIL's extractant capacity to form H bonds with MA. Superior values of extraction yield were obtained in the case of $[C_{14}C_6C_6C_6P][Dec]$, probably due to less sterical hindrance (decanoate being smaller than bis(2,4,4- tri-methyl-pentyl)phosphinate).

The reaction between MA and PILs was further investigated by FTIR analysis (Fig. 4c) of the extract compared to the organic phase. It proves the formation of hydrogen bonds between MA and PILs for both extractants, similar to citric acid and tri-octylamine extraction systems [35]: the OH (hydrogen-bonded) stretch valence oscillation around 3400–3500 $cm^{-1}$ domain can be detected,

**Table 2**
Loading factor values obtained for MA extraction.

| $[C_{14}C_6C_6C_6P][Dec]$ concentration | | Loading factor, Z | $[C_{14}C_6C_6C_6P][(iOc)_2Phos]$ concentration | | Loading factor, Z |
|---|---|---|---|---|---|
| M | g/L | – | M | g/L | – |
| 0.03 | 20 | 0.155 | 0.02 | 20 | 0.161 |
| 0.06 | 40 | 0.094 | 0.05 | 40 | 0.102 |
| 0.12 | 80 | 0.046 | 0.10 | 80 | 0.048 |
| 0.18 | 120 | 0.031 | 0.15 | 120 | 0.032 |

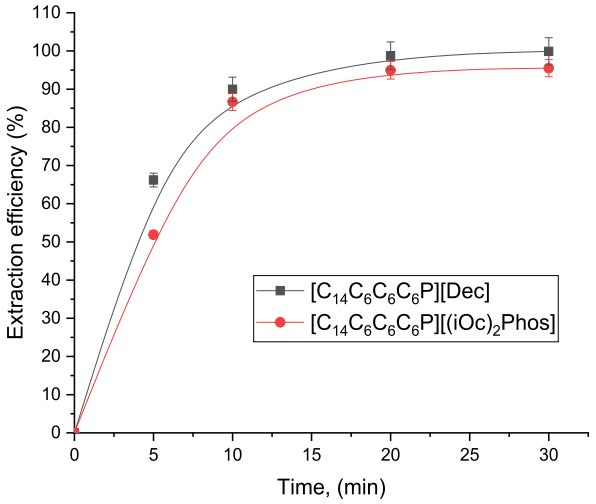


**Fig. 6.** Contact time influence on MA reactive extraction (0.8 g/L MA concentration, aqueous phase pH 3, 40 g/L PIls concentration).

and an increasing peak can be observed in the PILs extracts spectrum. The major peaks observed between 2800 and 3000 $cm^{-1}$ corresponding to H–C–H stretch are representative for heptane, while for ionic liquid peaks are mainly visible in the 1800-600 $cm^{-1}$ domain: at 1466 $cm^{-1}$ corresponding to P–C stretching, at 1382 $cm^{-1}$ to C - H in-plane bending, and the characteristic vibrations reflecting the presence of PIL anions: for $[C_{14}C_6C_6C_6P][(iOc)_2Phos]$: $POO^-$ at ca. 1026 $cm^{-1}$, P–$CH_2$ at ca. 1467 $cm^{-1}$ and COO- at ca. 1563 $cm^{-1}$ and ca. 1406 $cm^{-1}$; and for $[C_{14}C_6C_6C_6P][Dec]$: stretching vibration of C=O at ca. 1716 $cm^{-1}$. FTIR spectroscopy of the MA extract spectrum showed the presence of novel bands at around 1634–1636 $cm^{-1}$ (C=O stretching mode vibration) and at approximately 1559–1561 $cm^{-1}$ (carboxylate peak) [36,37].

Fig. 5 shows the extraction yield as a function of PILs concentration in the organic phase: an improved yield can be observed with the increased extractant concentration in the inert diluent, and the maximum MA extraction is observed at approximately 0.12 mol/L (80 g/L) for both ionic liquids, corresponding to the optimal composition of the organic phase. Visual observations showed no third-phase formation for any of the analysed systems. Reaching the optimum conditions at equilibrium for different extraction systems and achieving reproducible results requires understanding emulsification. It is crucial to prevent this undesirable phenomenon while preserving the PILs-diluent system's capacity for easy regeneration. The dilution of PILs with n-heptane is likely the primary cause of the high stability of this extraction system (depending on the polarity of the diluent used, it is incorporated preferentially in the polar or non-polar domains of the IL) and the short time required to reach high extraction efficiencies in the investigated system (hydrophobic ionic liquids based on tetradecyl-(trihexyl) phosphonium diluted with heptane), as no emulsification was observed.

The analysis of different extraction systems points out that the extraction system behaviour is very different for specific ILs/carboxylic acid systems. Zhang et al. (2021) removed 55%–88 % perfluorooctanoic acid (its specific hydrophobic and oleophobic properties lead to low extraction efficiency and severe emulsification) in diluted wastewater using [methyltrioctylammonium][bis(trifluoromethylsulfonyl)imide], and observed that ILs addition could suppress the emulsification with high extraction efficiency [38]. Grabda et al. (2022) obtained an extraction efficiency of 80 %–91 % for perfluorooctanoic acid from water by using [trihexyltetradecylphosphonium][pivalic acid] as IL, without emulsification difficulties developed for a particular PFOA: IL ration of 1:1 and re-extraction using a 1 % NaOH solution [39]. Marták and Schlosser (2019) investigated the reactive extraction of monocarboxylic acids using hydrophobic ionic liquids diluted with dodecane in a setup where equilibrium requires more than 10 h in a rotating shaking water bath. They observed coextraction of acid and water, and competitive extraction of acid and water, probably due to extremely high time necessary for reaching equilibrium [40].

PILs with a hydrophobic anion form complexes with MA through H bond formation at the interface between the organic and aqueous phase, with different stoichiometry: 1:1 (when a molecule of MA and PILs are involved in the complex formation), n:1 (when more molecules of MA react with one molecule of PILs for the complex formation) or 1:n (when a molecule of MA and more molecules

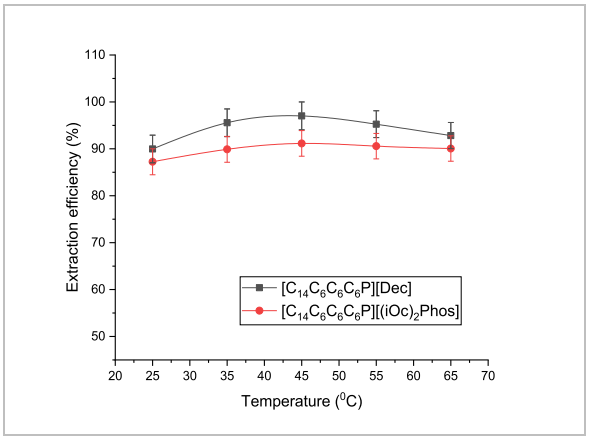


**Fig. 7.** Temperature influence on MA reactive extraction (0.8 g/L MA concentration, aqueous phase pH 3, 40 g/L PIls concentration).

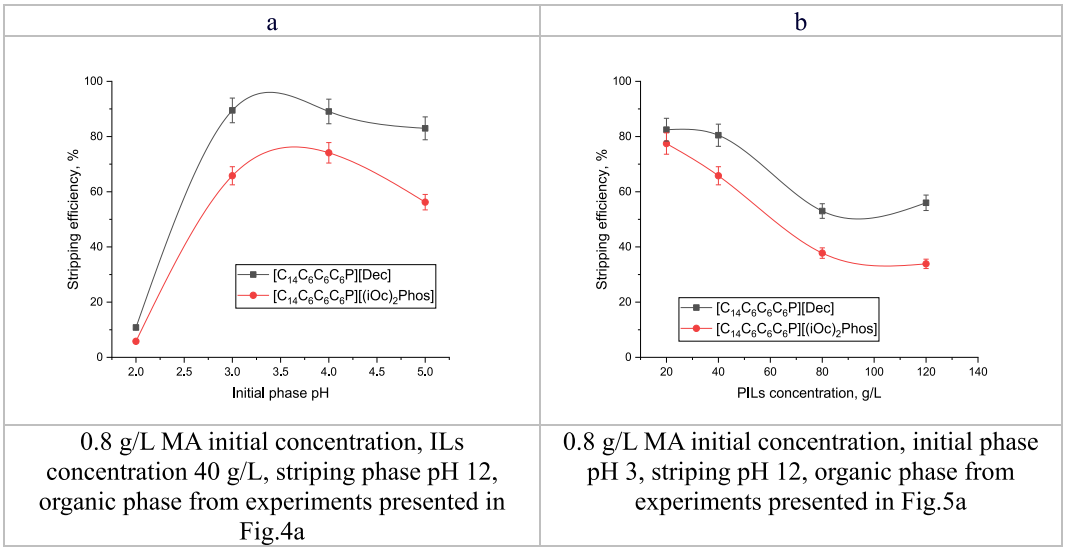


**Fig. 8.** Initial aqueous phase pH and PILs concentration on MA stripping (0.8 g/L MA initial concentration, final aqueous phase pH 12).

of PILs are involved in the complex formation).

To establish the number of molecules of MA and PILs involved in forming the hydrophobic complex, the loading ratio (Z, ($[MA]_{org}$/$[PIL]_{org}$) was calculated.

The results in Table 2 proved no overloading during the complex's formation, as evidenced by the loading ratio decreasing as PILs concentration increased and Z values below 1. This suggested the formation of an equimolecular complex including just one MA and one ionic liquid molecule.

Experiments were conducted for both PILs to examine the dependence of MA extraction efficiency on extraction time. The findings shown in Fig. 6 indicated that the maximum yield was reached for all systems after 10 min and stayed consistent during the whole investigation period. Good mixing conditions are necessary for reactive extraction as they help increase the contact between the solute and extractant, increasing the reaction rate. The optimum contact time (20 min) ensured intense mixing and intimate contact between the aqueous and organic phases, thus achieving equilibrium. These results are in accordance with findings obtained for muconic acid reactive extraction using amines [20].

Ionic liquids have a high viscosity by nature, and it has been observed that when temperature increases, the organic phase's viscosity decreases, improving mass transfer [41]. For MA, the extraction process was analysed at various temperatures between 25 and 65 °C using 40 g/L extractant at pH 3.0. Using PILs as extractants, MA extraction efficiency slowly decreased with the increase in temperature (Fig. 7). This phenomenon may be connected to MA back extraction in the aqueous phase, which appears at higher temperatures and reduces process efficiency overall. This parameter is of the lowest importance in the extraction process for the considered experimental domain.

Several studies have been conducted on the reactive extraction process of muconic acid. Demir et al. (2021) used tri-n-butyl

**Table 3**
Statistics for the determined models.

| | | Training | | | | | Testing | | | | |
|---|---|---|---|---|---|---|---|---|---|---|---|
| | | $R^2$ score | MAE | MSE | MAPE | $r^2$ | $R^2$ score | MAE | MSE | MAPE | $r^2$ |
| Case 1 | M5 adam | **0.990** | **1.231** | **2.380** | **0.017** | **0.990** | **0.987** | **1.628** | **5.375** | **0.041** | **0.987** |
| | M5 adamax | 0.973 | 1.577 | 6.430 | 0.020 | 0.973 | 0.960 | 2.423 | 16.754 | 0.052 | 0.960 |
| | M6-adam | 0.972 | 2.294 | 7.813 | 0.028 | 0.967 | 0.980 | 2.293 | 8.574 | 0.050 | 0.979 |
| | M6-adamax | 0.957 | 2.005 | 10.252 | 0.026 | 0.957 | 0.960 | 2.718 | 16.766 | 0.054 | 0.960 |
| Case 2 | M5 adam | **0.996** | **1.144** | **1.977** | **0.013** | **0.993** | **0.991** | **1.393** | **5.234** | **0.044** | **0.990** |

phosphate (TBP) in concentrations between 10 and 50 % by volume and tri-n-octyl phosphine oxide (TOPO) in concentrations between 4 % and 16 % by volume dissolved in different solvents (1-butanol, isoamyl alcohol, methyl ethyl ketone, methyl isobutyl ketone, di-isobutyl ketone, iso-butanol, hexane, diethyl carbonate). They obtained extraction degrees between 70 and 93 % at an MA concentration of 0.007 mol/kg [19]. Gorden et al. (2015) analysed tri-n-octyl amine, or TOA, dissolved in ethyl oleate and obtained a 95 % efficiency rate for MA reactive extraction. However, in this system, a third phase situated at the interface but inside the organic phase was seen to form. Several phase modifiers, including ethanol, 1-butanol, 1-pentanol, 1-octanol, and 1-dodecanol, were examined in an attempt to address this issue; only ethanol was shown to be unable to stop the creation of the third phase, while butanol use yielded in a 95.66 % extraction degree [23]. The results obtained in this study allowed superior values for extraction efficiency: 99.24 %.

### 3.2. Stripping

Recovering MA from the loaded organic phase is crucial in the context of reusing the ionic liquid and protecting the environment. This investigation analysed a combined approach for muconic acid recovery: pH modification of the stripping phase pH at 12 (NaOH solutions) and an increased temperature at 50 °C. Regardless of the pH of the starting phase or the extractant concentration, the results from Fig. 8 demonstrated a more effective stripping of MA in the case of $[C_{14}C_6C_6C_6P][Dec]$ compared to $[C_{14}C_6C_6C_6P][(iOc)_2Phos]$.

Because MA dissociates in the aqueous phase in correlation to its pH, and the fact that for breaking the equimolecular complex formed with the extractant, MA has to be converted into its undissociated form, back-extraction efficiency of MA is higher when carried out using an aqueous solution with a high pH when MA is converted into its sodium salt. The maximum efficiency for MA stripping from the loaded organic phase is achieved at an initial aqueous phase pH equal to 3 because the organic phase is loaded with the highest complex amount corresponding to maximum extraction efficiency for 40 g/L PILs in the organic phase. Nearly 89 % MA was recovered in a single contact from the loaded organic phase for organic: aqueous volume ratio of 1:1. The MA dissociated form corresponding to high pH does not possess the ability to form a complex with the PILs and is re-extracted into the aqueous phase. Regarding PILSs concentration influence on the stripping efficiency, from Fig. 8, it can be observed that the stripping process is more effective at low extractant concentrations in the organic phase, probably correlated with an increased viscosity of the organic phase due to the increased proportion of PILs.

The FTIR analysis (Supplementary material) was carried out to check the form of the extractant after stripping. Comparing the spectra, all characteristic peaks appeared PILs spectra after the stripping, confirming their stability. The stability and recycling capacity of PILs were evaluated to assess its utility as an extractant for practical purposes. PILs characteristics have been investigated for MA separation in terms of stripping efficiencies change as percent. The re-extraction efficiencies obtained were 84.47 %, 82.04 %, and 81.11 %, for $[C_{14}C_6C_6C_6P][Dec]$ and 61.47 %, 58.47 %, and 56.86 % for $[C_{14}C_6C_6C_6P][(iOc)_2Phos]$ for the recycled organic phase in the next three stages, which were close to the first extraction stage. The gradual decrease in extraction yields observed while employing the regenerated PILs can be explained by a small pH increase during sodium hydroxide back-extraction, which lowers extraction efficiency [42]. Regeneration, recovery, and reuse of PILs remain a major issue. Ionic liquids are more environmentally friendly than organic solvents due to their high boiling point, making it more challenging to distil them to produce pure products. Recovering ionic liquids at a lower cost and with less impact on the environment is a difficult undertaking. Further improvements are required for MA back-extraction from the organic phase.

### 3.3. Modeling and optimisation

The modelling strategy was performed considering two cases: i) with contact time; and ii) without. In the first case, the following parameters were used to model the extraction process: pH, extractant concentration, contact time, temperature, and type of extractant ($[C_{14}C_6C_6C_6P][Dec]$ or $[C_{14}C_6C_6C_6P][(iOc)_2Phos]$). For this model to be applied, preliminary equilibrium studies are needed to verify the influence of the contact time between phases, as the contact time for reaching equilibrium is strictly related to the mixing conditions (hydrodynamic conditions) used. In the second case, the model was determined using the same parameters as in the first case (except contact time). Since the extractant type is a discrete parameter, a coding procedure of the One-Hot-Encoding type was used, where each type of extractant has its corresponding specific column, and the use of the type is identified by the value 1. The Min-Max approach [43] was used to normalise the data. Preliminary tests have indicated that the process is complex and that the experimental data obtained in the laboratory need to be revised to identify an optimal model. Thus, an interpolation procedure was applied, where each combination of parameters was modelled with a regression relationship of order 3, and intermediate points were extracted. Therefore, the database was expanded from 30 data to 340 points (for case 1) and from 22 to 240 (for case 2). If the first case also

**Table 4**
Characteristics of the best models.

| | Layer (type) | Output Shape | Param # |
|---|---|---|---|
| Case 1 | dense_122 (Dense) | (None, 11) | 77 |
| | dense_123 (Dense) | (None, 8) | 96 |
| | dense_124 (Dense) | (None, 1) | 9 |
| | Total params: 182 | | |
| | Trainable params: 182 | | |
| | Non-trainable params: 0 | | |
| Case 2 | dense_626 (Dense) | (None, 17) | 102 |
| | dense_627 (Dense) | (None, 4) | 72 |
| | dense_628 (Dense) | (None, 8) | 40 |
| | dense_629 (Dense) | (None, 1) | 9 |
| | Total params: 671 | | |
| | Trainable params: 223 | | |
| | Non-trainable params: 0 | | |

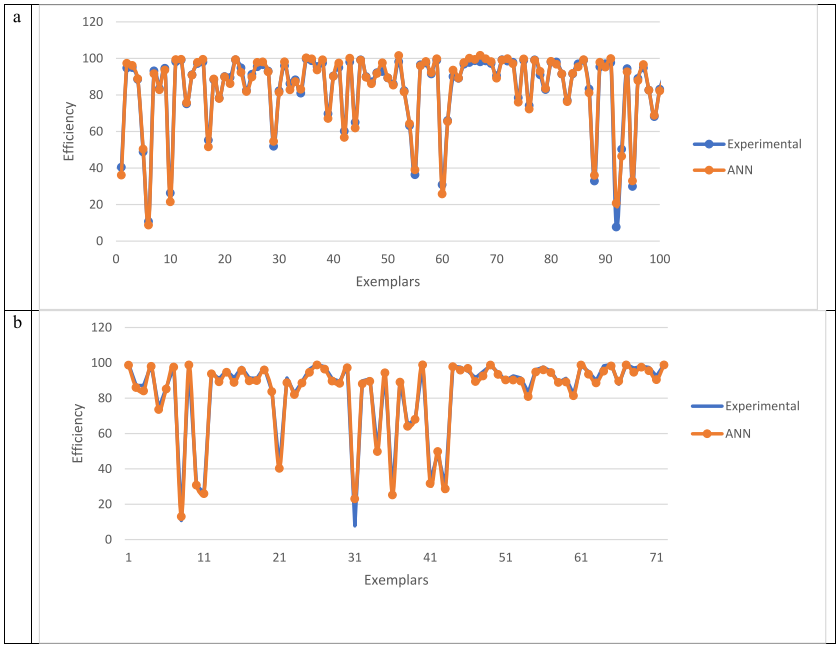


**Fig. 9.** Comparison of experimental and predicted data for a) case 1 and b) case 2.

considers a variation of contact time, the second case is determined only for a fixed contact time equal to 10 min. These were later used to determine the complete neural pattern. Statistical indicators for the best models obtained are presented in Table 3. After that, the best settings identified for case 1 were also applied in case 2.

In this table, M5 indicates a model with a limit of 5 hidden layers with limits of the maximum number of neurons set to Refs. [10,10,10,10,20], and M5 indicates a model with a maximum of 6 hidden layers with limits of [10,10,10,10,10,20]. $R^2$ score is the variation score, MAE is the mean absolute error, MSE is the mean square error, MAPE is the mean percentage absolute error, and $r^2$ is the coefficient of determination. The closer the $R^2$ score and $r^2$ are to 0, and the lower the MAE, MSE, and MAPE values, the higher the model's performance. As seen from Table 3, the Adam algorithm tends to give better results for the current process than Adamax. Regarding limits for the model structure, the variant with a maximum of 5 layers offers better results. This can be explained by the complexity of the search space, which increases with the number of layers, requiring a more significant number of iterations to identify an optimal pattern. Thus, the model identified as M5_Adam as the most suitable for the studied process was chosen.

The characteristics of the best models obtained in both cases are presented in Table 4. As can be seen, the best model for case 1 has two hidden layers, with 11 and 8 neurons respectively. On the other hand, the model for the second case is more complex and has 3 hidden layers with respectively 17, 4 and 8 neurons.

Fig. 9 compares experimental data with those predicted by the network. The differences are minimal in both cases, indicating that the neural model has learned the dynamics of the extraction process and can generate predictions.

An analysis of the importance of inputs to model outputs (identified by the Shap values [44]) is shown in Fig. 10. It is noted that the most important parameter is pH, for which small values tend to lead to an increase in output (small pH leads to a high yield). The next

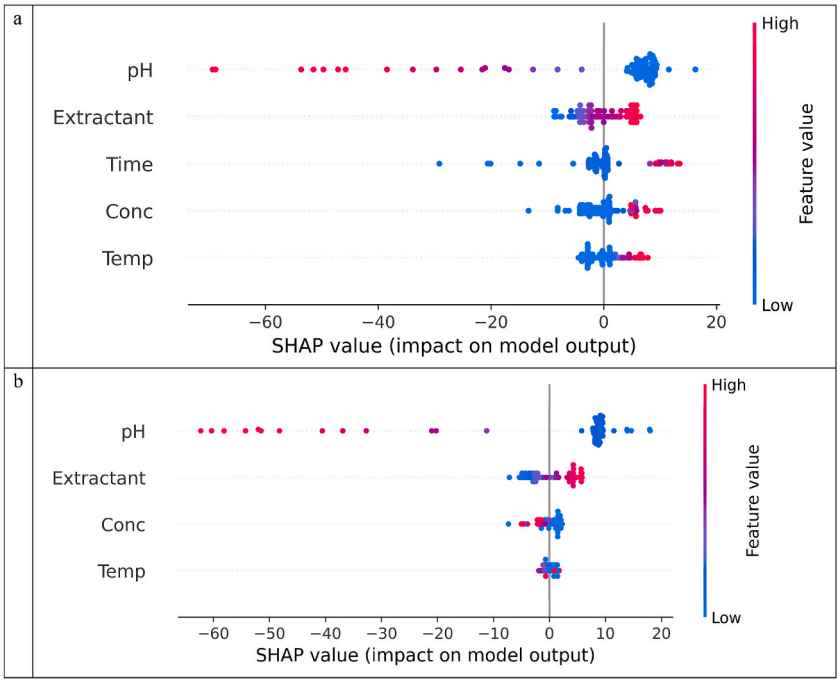


**Fig. 10.** Shap values a) case 1 and b) case 2.

**Table 5**
Optimisation results in case 1.

| $[C_{14}C_6C_6C_6P]$ [Dec] | $[C_{14}C_6C_6C_6P]$ $[(iOc)_2Phos]$ | pH | Extractant concentration (g/L) | Time (min) | Temperature (°C) | Extraction efficiency (%) |
|---|---|---|---|---|---|---|
| 0 | 1 | 3.9 | 55.09 | 23.24 | 53.65 | 102.3 |
| 0 | 1 | 3.29 | 73.91 | 26.65 | 50.03 | 101.71 |
| 1 | 0 | 4.8 | 51.52 | 25.94 | 55.31 | 101.37 |
| 0 | 1 | 3.63 | 54.17 | 23.12 | 43.91 | 101.34 |
| 0 | 1 | 4.16 | 90.44 | 21.57 | 35.42 | 100.52 |
| 0 | 1 | 4.11 | 87.33 | 25.84 | 25.3 | 99.83 |
| 0 | 1 | 2.43 | 81.15 | 28.79 | 59.9 | 99.53 |
| 0 | 1 | 4.11 | 87.33 | 25.21 | 25.3 | 99.27 |
| 1 | 0 | 4.25 | 64.55 | 22.01 | 38.92 | 99.24 |
| 0 | 1 | 4.00 | 97.83 | 21.66 | 54.03 | 99.14 |
| 0 | 1 | 4.27 | 60.55 | 25.84 | 39.33 | 99.17 |
| 0 | 1 | 3.97 | 74.59 | 23.23 | 26.23 | 98.92 |
| 0 | 1 | 2.11 | 81.15 | 28.79 | 63.26 | 98.28 |
| 0 | 1 | 2.36 | 45.09 | 25.54 | 20.49 | 97.95 |
| 0 | 1 | 3.97 | 83.18 | 23.23 | 20.91 | 97.95 |
| 0 | 1 | 3.74 | 45.45 | 20.91 | 65.00 | 97.47 |
| 0 | 1 | 4.25 | 34.88 | 21.76 | 42.95 | 96.91 |
| 1 | 0 | 3.38 | 38.66 | 23.87 | 30.71 | 96.69 |
| 1 | 0 | 3.38 | 38.66 | 23.87 | 33.07 | 95.73 |
| 0 | 1 | 4.81 | 117.34 | 24.24 | 38.02 | 95.65 |
| 0 | 1 | 4.26 | 67.37 | 25.17 | 30.92 | 95.61 |
| 0 | 1 | 2.1 | 79.59 | 25.15 | 60.06 | 95.57 |
| 1 | 0 | 3.38 | 38.66 | 24.08 | 33.07 | 95.47 |
| 1 | 0 | 3.38 | 38.66 | 24.08 | 33.07 | 95.47 |
| 1 | 0 | 4.8 | 51.52 | 26.54 | 44.32 | 95.07 |

important parameter is the extractant, followed by Time (in case 1) and Concentration (in case 2). Temperature is the parameter with the least influence on the model. Overall, it can be observed that the elimination of contact time from the model does not change the impact of parameters on the output. Nevertheless, if for case 1 it can be observed clearly that increasing the temperature tends to result in a slight increase in efficiency, this is not applicable for case 2, where there is no clear distinction between the impact of low and high values for temperature.

In the final step, the best model obtained in combination with the same DE algorithm is used to optimize the process. Tables 5 and 6 present a set of process parameters that lead to high extraction efficiency.

**Table 6**
Optimisation results in case 2.

| $[C_{14}C_6C_6C_6P]$ [Dec] | $[C_{14}C_6C_6C_6P]$ $[(iOc)_2Phos]$ | pH | Extractant concentration (g/L) | Temperature (°C) | Extraction efficiency (%) |
|---|---|---|---|---|---|
| 0 | 1 | 2.67 | 65.06 | 26.19 | 103.33 |
| 1 | 0 | 2.42 | 61.64 | 29.62 | 103.3 |
| 1 | 0 | 2.34 | 99.35 | 25.11 | 103.11 |
| 0 | 1 | 2.67 | 65.06 | 27.51 | 102.92 |
| 1 | 0 | 2.22 | 120 | 27.88 | 102.61 |
| 1 | 0 | 2.69 | 60.27 | 20.82 | 101.81 |
| 1 | 0 | 2.77 | 43.95 | 23.41 | 99.74 |
| 1 | 0 | 2.41 | 97.29 | 30 | 99.71 |
| 1 | 0 | 2.6 | 104.59 | 22.45 | 99.32 |

As observed, the extraction efficiency is higher than 100 % in some cases. The error introduced by the model can explain this, as no hard limits were set for the output during the optimisation phase. For the process parameters, the experimental limits are kept unchanged.

In case 1, the optimisation results show that both extractants can be highly efficient; the optimisation step does not favour a particular one. Moreover, the combinations of parameters are not focused on a particular set of values, indicating that the search space is complex and the DE algorithm was able to explore it efficiently.

In case 2, the solutions are somewhat closer, indicating that the process has a reduced pool of local optima.

## 4. Conclusions

A new extraction technique utilising hydrophobic ILs was investigated in this work to effectively extract muconic acid from aqueous solutions, such as fermentation broth. The findings demonstrated that the best extraction conditions for MA were pH = 3.0, 20 min contact time, 45 °C temperature, and above 40 g/L ionic liquid dissolved in heptane when using $[C_{14}C_6C_6C_6P][Dec]$ as the extractant. Additionally, an analysis of the extraction system's mechanism revealed an equimolecular hydrophobic complex between PILs and MA for both extractants examined. Low stripping efficiency compared to extraction efficiency was observed, so further investigation on the influence of stripping phase pH, contact time and temperature are required to improve stripping method efficiency. ANNs and DE algorithms were used to model and optimize the process, and the results obtained indicated that the selected approach could find a suitable model that can be further used to identify combinations of process parameters that lead to a high extraction efficiency.

## Data availability

Data will be made available on request.

## CRediT authorship contribution statement

**Alexandra Cristina Blaga:** Writing – review & editing, Writing – original draft, Supervision, Project administration, Funding acquisition, Conceptualization. **Elena Niculina Dragoi:** Writing – review & editing, Software, Formal analysis. **Alexandra Tucaliuc:** Writing – review & editing, Visualization, Methodology, Formal analysis. **Lenuta Kloetzer:** Visualization, Validation, Investigation. **Adrian-Catalin Puitel:** Formal analysis. **Dan Cascaval:** Writing – review & editing, Validation, Supervision, Resources, Data curation. **Anca Irina Galaction:** Writing – review & editing, Visualization, Validation, Funding acquisition.

## Declaration of competing interest

The authors declare that they have no known competing financial interests or personal relationships that could have appeared to influence the work reported in this paper.

## Acknowledgement

This work was supported by a grant from the Ministry of Research, Innovation and Digitization, CNCS - UEFISCDI, project number PN-III-P1-1.1-TE-2021-0153, within PNCDI III and CNFIS-FDI-2024-F-0099.

## Appendix A. Supplementary data

Supplementary data to this article can be found online at https://doi.org/10.1016/j.heliyon.2024.e36113.

## References


[1] Menglei Li, Jiayao Chen, Keqin He, Changsheng Su, Yilu Wu, Tianwei Tan, Corynebacterium glutamicum cell factory design for the efficient production of cis, cis-muconic acid, Metab. Eng. 82 (2024) 225–237, https://doi.org/10.1016/j.ymben.2024.02.005.

[2] Jingjing He, Yongjun Jiang, Bingjie Ding, Yajun Wang, Hewen Qiu, Sheng Dai, Xiuge Zhao, Zhenshan Hou, Zirconium phosphate supported copper catalyst for selective oxidation of phenol to cis, cis-muconic acid, Appl. Catal. Gen. 664 (2023) 119351, https://doi.org/10.1016/j.apcata.2023.119351.

[3] Sridevi Veluru, Ramakrishna Seeram, Biotechnological approaches: degradation and valorization of waste plastic to promote the circular economy, Circular Economy 3 (1) (2024) 100077, https://doi.org/10.1016/j.cec.2024.100077.

[4] C. Ling, G.L. Peabody, D. Salvachúa, et al., Muconic acid production from glucose and xylose in *Pseudomonas putida* via evolution and metabolic engineering, Nat. Commun. 13 (2022) 4925, https://doi.org/10.1038/s41467-022-32296-y.

[5] Robert S. Nelson, Eric P. Knoshaug, Ryan Spiller, Nick Nagle, Stefanie VanWychen, Matthew Wiatrowski, Ryan Davis, Philip T. Pienkos, Jacob S. Kruger, Muconic acid production from algae hydrolysate as a high-value co-product of an algae biorefinery, Algal Res. 75 (2023) 103300, https://doi.org/10.1016/j.algal.2023.103300.

[6] M.E. Pyne, L. Narcross, M. Melgar, K. Kevvai, S. Mookerjee, G.B. Leite, V.J.J. Martin, An engineered Aro1 protein degradation approach for increased cis,cis-muconic acid biosynthesis in Saccharomyces cerevisiae, Appl. Environ. Microbiol. 84 (17) (2018), https://doi.org/10.1128/AEM.01095-18.

[7] G. Wang, A. Tavares, S. Schmitz, L. França, H. Almeida, J. Cavalheiro, A. Carolas, S. Øzmerih, L.M. Blank, B.S. Ferreira, I. Borodina, An integrated yeast-based process for cis,cis-muconic acid production, Biotechnol. Bioeng. 119 (2) (2021) 376–387, https://doi.org/10.1002/bit.27992.

[8] B. Thompson, S. Pugh, M. Machas, D.R. Nielsen, Muconic acid production via alternative pathways and a synthetic "metabolic funnel", ACS Synth. Biol. 7 (2) (2017) 565–575, https://doi.org/10.1021/acssynbio.7b00331.

[9] R. Fujiwara, S. Noda, T. Tanaka, A. Kondo, Muconic acid production using gene-level fusion proteins in Escherichia coli, ACS Synth. Biol. 7 (11) (2018) 2698–2705, https://doi.org/10.1021/acssynbio.8b00380.

[10] H.-N. Lee, W.-S. Shin, S.-Y. Seo, S.-S. Choi, J. Song, J. Kim, J. Park, D. Lee, S.Y. Kim, S.J. Lee, G.-T. Chun, E.-S. Kim, Corynebacterium cell factory design and culture process optimization for muconic acid biosynthesis, Sci. Rep. 8 (2018) 18041, https://doi.org/10.1038/s41598-018-36320-4.

[11] S. Wang, M. Bilal, Y. Zong, H. Hu, W. Wang, X. Zhang, Development of a plasmid-free biosynthetic pathway for enhanced muconic acid production in Pseudomonas chlororaphis HT66, ACS Synth. Biol. 7 (5) (2018) 1131–1142, https://doi.org/10.1021/acssynbio.8b00047.

[12] C. Ling, G.L. Peabody, D. Salvachúa, Y.-M. Kim, C.M. Kneucker, C.H. Calvey, M.A. Monninger, N.M. Munoz, B.C. Poirier, K.J. Ramirez, P. C. St John, S. P. Woodworth, J.K. Magnuson, K.E. Burnum-Johnson, A.M. Guss, C.W. Johnson, G.T. Beckham, Muconic acid production from glucose and xylose in Pseudomonas putida via evolution and metabolic engineering, Nat. Commun. 13 (2022) 4925, https://doi.org/10.1038/s41467-022-32296-y.

[13] H.-M. Jung, M.-Y. Jung, M.-K. Oh, Metabolic engineering of Klebsiella pneumoniae for the production of cis,cis-muconic acid, Appl. Microbiol. Biotechnol. 99 (2015) 5217–5225, https://doi.org/10.1007/s00253-015-6442-3.

[14] M.E. Pyne, J.A. Bagley, L. Narcross, K. Kevvai, K. Exley, M. Davies, Q. Wang, M. Whiteway, V.J.J. Martin, Screening non-conventional yeasts for acid tolerance and engineering Pichia occidentalis for production of muconic acid, Nat. Commun. 14 (2023) 5294, https://doi.org/10.1038/s41467-023-41064-5.

[15] N. Yoshikawa, S. Mizuno, K. Ohta, M. Suzuki, Microbial production of cis, cis-muconic acid, J. Biotechnol. 14 (1990) 209–210, https://doi.org/10.1016/0168-1656(90)90009-Z.

[16] M. Kohlstedt, S. Starck, N. Barton, J. Stolzenberger, M. Selzer, K. Mehlmann, R. Schneider, D. Pleissner, J. Rinkel, J.S. Dickschat, et al., From lignin to nylon: cascaded chemical and biochemical conversion using metabolically engineered Pseudomonas putida, Metab. Eng. 47 (2018) 279–293, https://doi.org/10.1016/j.ymben.2018.03.003.

[17] V. Inyang, D. Lokhat, Reactive extraction of malic acid using trioctylamine in 1–decanol: equilibrium studies by response surface methodology using Box behnken optimization technique, Sci. Rep. 10 (2020) 2400, https://doi.org/10.1038/s41598-020-59273-z.

[18] D. Małgorzata, H. Marek, Reactive extraction of carboxylic acids using organic solvents and supercritical fluids: a review, Separ. Purif. Technol. 201 (2018) 106–119, https://doi.org/10.1016/j.seppur.2018.02.010.

[19] Ö. Demir, A. Gök, H. Uslu, Ş.İ. Kırbaşlar, Reactive extraction of cis,cis-muconic acid from aqueous solution using phosphorus-bonded extractants, tri-n-octylphosphineoxide and tri-n-butyl phosphate: equilibrium and thermodynamic study, Sep. Purif. Technol. 272 (2021) 118899, https://doi.org/10.1016/j.seppur.2021.118899.

[20] A. Bahrami, F. Ghamari, Y. Yamini, F.G. Shahna, A. Koolivand, Ion-pair-based hollow-fiber liquid-phase microextraction combined with high-performance liquid chromatography for the simultaneous determination of urinary benzene, toluene, and styrene metabolites, J. Separ. Sci. 41 (2018) 501, https://doi.org/10.1002/jssc.201700685.

[21] S. Abbaszadeh, S. Yousefinejad, S. Jafari, E. Soleimani, In-syringe ionic liquid-dispersive liquid-liquid microextraction coupled with HPLC for the determination of trans,trans-muconic acid in human urine sample, J. Separ. Sci. 44 (2021) 3126, https://doi.org/10.1002/jssc.202100044.

[22] S. Tönjes, E. Uitterhaegen, P. De Brabander, E. Verhoeven, T. Delmulle, K. De Winter, W. Soetaert, In situ product recovery as a powerful tool to improve the fermentative production of muconic acid in *Saccharomyces cerevisiae*, Biochem. Eng. J. 190 (2023) 108746, https://doi.org/10.1016/j.bej.2022.108746.

[23] J. Gorden, T. Zeiner, C. Brandenbusch, Reactive extraction of cis,cis-muconic acid, Fluid Phase Equil. 393 (2015) 78–84, https://doi.org/10.1016/j.fluid.2015.02.030.

[24] M. Blahusiak, S. Schlosser, J. Martak, Extraction of butyric acid with a solvent containing ammonium ionic liquid, Sep. Purif. Technol. 19 (2013) 102–111, https://doi.org/10.1016/j.seppur.2013.09.005.

[25] J. Marták, Š. Schlosser, Phosphonium ionic liquids as new, reactive extractants of lactic acid, Chem. Pap. 60 (5) (2006) 395–398, https://doi.org/10.2478/s11696-006-0072-2.

[26] J. Marták, Š. Schlosser, New mechanism and model of butyric acid extraction by phosphonium ionic liquid, J. Chem. Eng. Data 61 (9) (2016) 2979–2996, https://doi.org/10.1021/acs.jced.5b01082.

[27] S.V. Prabhu, V. Varadharajan, S. Mohanasundaram, S. Manivannan, J.M. Khaled, M. Goel, K. Srihari, A comparative study on process optimization of betalain pigment extraction from Beta vulgaris subsp. vulgaris : RSM, ANN, and hybrid RSM-GA methods, Biomass Conversion and Biorefinery (2023), https://doi.org/10.1007/s13399-023-04581-3.

[28] S. Shekhar, P. Prakash, P. Singha, K. Prasad, S.K. Singh, Modeling and optimization of ultrasound-assisted extraction of bioactive compounds from Allium sativum leaves using response surface methodology and artificial neural network coupled with genetic algorithm, Foods 12 (2023), https://doi.org/10.3390/foods12091925.

[29] S. Hilali, L. Wils, A. Chevalley, B. Clément-Larosière, L. Boudesocque-Delaye, Glycerol-based NaDES as green solvents for ultrasound-assisted extraction of phycocyanin from Arthrospira platensis—RSM optimization and ANN modelling, Biomass Conversion and Biorefinery 12 (2022) 157–170, https://doi.org/10.1007/s13399-021-02263-6.

[30] G.E. Lee, R.H. Kim, T. Lim, J. Kim, S. Kim, H.G. Kim, K.T. Hwang, Optimization of accelerated solvent extraction of ellagitannins in black raspberry seeds using artificial neural network coupled with genetic algorithm, Food Chem. 396 (2022) 133712, https://doi.org/10.1016/j.foodchem.2022.133712.

[31] R.G. Lazar, A.C. Blaga, E.N. Dragoi, A.I. Galaction, D. Cascaval, Application of reactive extraction for the separation of pseudomonic acids: influencing factors, interfacial mechanism, and process modelling, Can. J. Chem. Eng. 100 (2021), https://doi.org/10.1002/cjce.24124.

[32] D.H. Wolpert, W.G. Macready, No free lunch theorems for optimization, IEEE T Evol Comput 1 (1997) 67–82, https://doi.org/10.1109/4235.585893.

[33] E.N. Dragoi, S. Curteanu, A.I. Galaction, D. Cascaval, Optimization methodology based on neural networks and self-adaptive differential evolution algorithm applied to an aerobic fermentation process, Appl. Soft Comput. 13 (1) (2013) 222–238, https://doi.org/10.1016/j.asoc.2012.08.004.

[34] I. Khalil, G. Quintens, T. Junker, M. Dusselier, Muconic acid isomers as platform chemicals and monomers in the biobased economy, Green Chem. 22 (2020) 1517–1541, https://doi.org/10.1039/C9GC04161C.

[35] L. Nolte, M. Nowaczyk, C. Brandenbusch, Monitoring and investigating reactive extraction of (di)carboxylic acids using online FTIR – Part I: Characterization of the complex formed between itaconic acid and tri-n-octylamine, J. Mol. Liq. 352 (2022) 118721, https://doi.org/10.1016/j.molliq.2022.118721.

[36] H. Beneš, J. Kredatusová, J. Peter, S. Livi, S. Bujok, E. Pavlova, J. Hodan, S. Abbrent, M. Konefał, P. Ecorchard, Ionic liquids as delaminating agents of layered double hydroxide during in-situ synthesis of poly (butylene adipate-co-terephthalate) nanocomposites, Nanomaterials 9 (4) (2019) 618, https://doi.org/10.3390/nano9040618.
[37] V.R. Dhongde, B.S. De, K.L. Wasewar, Experimental study on reactive extraction of malonic acid with validation by Fourier Transform Infrared Spectroscopy, J. Chem. Eng. Data 64 (3) (2019) 1072–1084, https://doi.org/10.1021/acs.jced.8b00972.
[38] K. Zhang, D. Kujawski, C. Spurrell, D. Wang, J. Yan, J.C. Crittenden, Extraction of PFOA from dilute wastewater using ionic liquids that are dissolved in n-octanol, J. Hazard Mater. (2021) 124091, https://doi.org/10.1016/j.jhazmat.2020.124091.
[39] M. Grabda, M. Zawadzki, S. Oleszek, M. Matsumoto, M. Królikowski, Y. Tahara, Removal of perfluorooctanoic acid from water using a hydrophobic ionic liquid selected using the conductor-like screening model for realistic solvents, Environ. Sci. Technol. 56 (10) (2022) 6445–6454, https://doi.org/10.1021/acs.est.1c08537.
[40] J. Marták, Š. Schlosser, Influence of anion and cation structure of ionic liquids on carboxylic acids extraction, Front. Chem. 7 (2019) 117, https://doi.org/10.3389/fchem.2019.00117.
[41] B.B. Mishra, N. Devi, K. Sarangi, Solvent extraction and separation of samarium from transition and rare-earth metals using phosphonium ionic liquid Cyphos IL 104, Monatsh. Chem. 152 (2021) 767–775, https://doi.org/10.1007/s00706-021-02792-w.
[42] A.F.M. Cláudio, A.M. Ferreira, C.S.R. Freire, A.J.D. Silvestre, M.G. Freire, J.A.P. Coutinho, Sep. Purif. Technol. 97 (2012) 142, https://doi.org/10.1021/jp204865a.
[43] D. Fryer, I. Strümke, H. Nguyen, Shapley values for feature selection: the good, the bad, and the axioms, IEEE Access 9 (2021) 144352–144360, https://doi.org/10.1109/ACCESS.2021.3119110.
[44] K. Priddy, P. Keller, Artificial Neural Networks:An Introduction, SPIE Press, Washington, 2005.